YAEC-1071

YANKEE ROWE CORE XI

DECAY HEAT REDISTRIBUTION FACTOR DURING SHUTDOWN CONDITIONS

By
John N. Hamawi
Research & Engineering Development

June 1974

Prepared By John N. Hamawi 6/20/74 (Date)

Reviewed By W. D. Hinkle 7/1/74 (Date)

Approved By W. D. Hinkle 7/1/74 (Date)

Yankee Atomic Electric Company
20 Turnpike Road
Westboro, Massachusetts 01581

DISCLAIMER OF RESPONSIBILITY

This document was prepared by Yankee Atomic Electric Company for its own use. It is being made available to others as a public service without monetary or other compensation to Yankee, upon the express understanding that neither Yankee Atomic Electric Company or any of its officers, directors, agents or employees assumes any obligation, responsibility or liability, or makes any warranty or representation, with respect to the contents of this document or its accuracy or completeness.

ABSTRACT

Due to the penetrating power of gamma photons and their long mean free paths compared to fuel rod dimensions, the gamma heating distribution in a reactor core is normally flatter than that of the gamma source. The degree of flattening is referred to as the decay heat redistribution factor. This report describes the determination of this factor for Core XI of the Yankee nuclear power station at Rowe, Massachusetts, under shutdown conditions. The analysis was based on the use of SHADRAC, a shield heating and dose rate attenuation code utilizing a moments-method solution of the Boltzmann transport equation. The model employed in the analysis is described in detail.

TABLE OF CONTENTS

LIST OF FIGURES

LIST OF TABLES

ACKNOWLEDGEMENTS

The author wishes to thank Dr. W. D. Hinkle for his guidance and helpful discussions in the course of this project. His careful review of the results and the report is appreciated. Special thanks are also extended to Virginia Mitchell and Jacquelyn Thompson for typing the original and final drafts of this report.

1.0 INTRODUCTION

Decay heat energy in a reactor core during shutdown conditions is composed of beta particles and gamma photons from the decay of fission and activation products. For normal design calculations both photons and particles are conservatively assumed to be captured at their point of origin. This assumption is valid only for beta particle absorption because of the short range these particles have in heavy material; the assumption, in fact, is still conservative since some beta energy will escape the fuel rod by bremsstrahlung radiation. The gamma photons on the other hand have considerably longer mean free paths relative to the fuel rod dimensions and can therefore escape from a fuel rod where they are generated and deposit their energies in the clad, moderator, structural and control materials or other adjacent or distant fuel rods. As a result, the gamma heating distribution at any particular location in the core is flatter than the gamma source distribution. In fact, the distributions would be similar only in cases where a given fuel rod gets back as much gamma energy as it loses, as would be the case, for instance, in a uniform array of rods in a flat power distribution and a very low density medium. Generally, however, the effect, which is often referred to as gamma smearing, results in a more diffuse gamma heat source.

The importance of gamma smearing, which is evaluated in terms of a decay heat redistribution factor, depends on the conditions being examined. For instance, the effect is more important during shutdown than during normal operation since during shutdown the gamma photons make up approximately 50 percent of the total energy, compared to approximately 11 percent during normal operation. But, of particular interest is the considerable reduction in peak clad temperatures that

can be achieved by accounting for this effect in the analysis of a loss-of-coolant accident.

Peak energy production in a fuel pin depends, in part, on localized geometric effects producing local thermal neutron flux peaking. In present PWR designs, this is caused largely by water holes designed to accommodate control rod fingers. The resulting local peaking used in design calculations is of the order of 6 to 10 percent (much greater in the case of cruciform rods), and occurs predominantly in the pins immediately adjacent to the water holes. But for LOCA calculations, where the energy source is from radioactive decay, local peaking factors decrease by approximately one-half down to 3 to 5 percent as a result of gamma smearing. In essence, as discussed in Sec. 2.5, the local peaking factor for the gamma half of the decay energy approaches unity and the gamma heating distribution becomes approximately flat. The exact amount of the reduction in peak fuel pin heat production from decay sources depends on the core design. Detailed calculations by the reactor suppliers during the rulemaking hearings on the ECCS Interim Acceptance Criteria lead to the following results (Ref. 1):

Manufacturer	Reduction Factor (%)
Combustion Engineering	6
Westinghouse	5
B & W	4

The Combustion design has a larger control rod water hole. This leads to a somewhat larger local peaking design value and therefore to a greater effect from decay heat redistribution. Combustion's cruciform rod design of Palisades has, of course, an even larger effect.

For the Yankee Rowe core, where the cruciform control rod configuration leads to local peaking factors* of the order of 1.3 to 1.4 (depending on the size of the fuel rod ensemble considered) the expected reduction is about 15 to 20 percent. An analysis carried out by Westinghouse and reported in the original Yankee Rowe FHSR (Ref. 2) indicates that the difference in F_Q^N (the nuclear heat flux factor) between steady state and shutdown condition is approximately 17 percent. Indeed, it is the scope of this work to develop a method and obtain an accurate value for this reduction.

---

*Local peaking factor is defined as the ratio of peak rod power to average power of rods in a given ensemble. The ensemble includes all rods (about 150) around the peak rod within a few mean free paths of the most penetrating gamma photons in the source spectrum. Rods beyond this emsemble are assumed to have no effect on the peak rod gamma heating.

2.0 ANALYTICAL MODEL

2.1 Redistribution Factors

The decay heat redistribution factor is defined as:

$$F = \frac{H}{G} \tag{1}$$

where G and H are the rates at which decay heat is generated and absorbed (respectively) per unit length of a fuel rod during shutdown conditions.

Since the decay heat source consists of both beta particles and gamma photons, it is important to account for these two types of radiation separately. Thus, if the fractional decay heat generation attributable to gamma rays is denoted by γ, then G and H can be put in the forms:

$$G = G\ (1 - \gamma) + G\gamma \tag{2}$$

and

$$H = G\ (1 - \gamma)\ F_{\beta} + G\gamma F_{\gamma} \tag{3}$$

where F_{β} and F_{γ} are the beta and gamma redistribution factors respectively. Therefore,

$$F = (1 - \gamma)\ F_{\beta} + \gamma F_{\gamma}. \tag{4}$$

Note that the redistribution factor is a function of position in the core. To compute F throughout the core is an almost impossible job. In this analysis, therefore, attention was focused only to the hottest spot in the core since this is the spot of primary concern in the evaluation of peak clad temperature following a postulated LOCA. Redistribution factors for a few rods surrounding the peak rod were also computed, but the analysis in this case was based on a rule-of-thumb approach described in Sec. 2.5.

It was noted in the introduction that the beta redistribution factor F_{β} is equal to unity since all beta particles are assumed absorbed at their

points of origin. It follows then that

$$F = 1 - \gamma(1-F_\gamma). \tag{5}$$

Also, since data for the gamma contribution to the total decay heat is available in the literature (Ref. 3), the only unknown in Eq. (5) is F_γ. This parameter is defined as

$$F_\gamma = \frac{H_\gamma}{G_\gamma} \tag{6}$$

where, since our primary interest is in the peak rod,

H_γ = gamma decay heat absorbed by the peak rod per unit length,

and $G_\gamma = \gamma G$ = gamma decay heat generated by the peak rod per unit length. The generated heat G_γ can be obtained from core design analyses and is equal to

$$G_\gamma = \gamma\ P_o\ \ P_i\ \ P_a\ \ \left\{ 1.2 \left[\frac{P}{P_o}\right]_{ANS} \right\} \tag{7}$$

where P_o is the core average linear heat generation rate,

P_i the radial peaking factor, and

P_a the axial peaking factor.

The last term in curly brackets is the normalized ANS decay heat standard with an added 20% uncertainty.

Evaluation of H_γ, on the other hand, is more elaborate since one must perform an energy dependent three dimensional integration that accounts for all gamma sources and their associated spectra. In addition, H_γ must be computed with appreciable accuracy since, as shown by Eq. (40) developed later, a 10% error in this parameter (or F_γ) is approximately equal to a 5% error in the total redistribution factor Γ. An error of this magnitude would significantly reduce the benefits that can be gained from the gamma

smearing effect.

Equations (5) and (6) and the methods described above are what is normally employed for the evaluation of redistribution factors. The approach requires the computation of both H_γ and G_γ on an absolute basis, a requirement that makes the evaluation of F with only a few percent error very difficult. However, the error in F_γ can be reduced if both H_γ and G_γ were computed on a relative (instead of absolute) basis using the same analytical model for both parameters. If this could be accomplished then the errors in H_γ and G_γ would tend to cancel out and would not be reflected in the H_γ/G_γ ratio.

Conversion from an absolute basis to a relative basis was accomplished using the following reasoning. Consider a large uniform array of long, activated rods immersed in a coolant and assume that all rods are equally and uniformly activated such that the source intensity per unit length of rod is independent of rod or position along a rod axis. At the center of this system all the gamma rays produced by the rods are absorbed by the rods and the coolant since these gamma rays cannot escape from the system in view of the assumed large dimensions of the latter. That is, at the center of the system, the heat generated per unit length of a rod is equal to the heat absorbed by a unit length of a rod-coolant cell, or

$$G_\gamma = \bar{H}_\gamma + \bar{H}_c \qquad (8)$$

where subscript c refers to the coolant and the barred symbols represent

the uniformly activated rods in the uniform matrix. Analysis of the results presented in Sec. 4.2 has shown that Eq. (8) is satisfied at the center of a spherical system with a radius equal to approximately 20 cm. Hence, without any approximation at this point, Eq. (6) can be rewritten as:

$$F_\gamma = \frac{H_\gamma}{\bar{H}_\gamma + \bar{H}_c} \quad . \tag{9}$$

Note that F_γ has a maximum value of unity (corresponding to the case where the gamma heat produced by the rod is equal to the heat it absorbs) and that any approximation in the analytical model that tends to increase the value of F_γ is necessarily conservative. Hence, since $\bar{H}_c$ in Eq. (9) amounts to only a few percent of G_γ, F_γ can be conservatively approximated by

$$F_\gamma = \frac{H_\gamma}{\bar{H}_\gamma} \quad . \tag{10}$$

This equation represents the ratio of heat absorbed per unit length of the peak rod in an actual core to that absorbed by an identical rod in a uniform matrix. The equation implies that there is no gamma smearing in a uniform array of equal-powered rods even if the rods are immersed in a coolant. Physically this is true only with a zero-density coolant.

To proceed further, when the heating contributions of the various rods around the peak rod are considered separately, Eq. (10) takes the form:

$$F_\gamma = \frac{\sum_{i=1}^{n} k_i \, h_i}{\sum_{i=1}^{n} \bar{h}_i} \tag{11}$$

where h_i and $\bar{h}_i$ are the heats absorbed per unit length of the peak rod from gamma rays emanating from rod i, and k_i is the rod peaking factor relative to the peak rod. Note that for the peak rod, i = 1 and $k_1 = 1$, and that for all other rods k_i is less than unity. In addition, since a number of the rods in the assumed uniform array are replaced by control rods or blades in the actual core configuration, some k_i values are equal to zero.

The application of Eq. (11) requires that similar geometrical arrangements be used for the evaluation of both H_γ and $\bar{H}_\gamma$. In fact, the only difference in the two geometries should be the replacement of a few rods in the uniform array by control rods or blades. In this way, h_i and $\bar{h}_i$ in Eq. (11) would be different only in the presence of some control material between rod i and the peak rod.

As a final remark, note that if the normally continuous gamma spectrum is assumed composed of a set of monoenergetic sources of specified energy and intensity, the equation for the redistribution factor takes the form

$$F_\gamma = \frac{\sum_j H_j(E)\, S_j(E)}{\sum_j \bar{H}_j(E)\, S_j(E)} \quad . \tag{12}$$

In this expression H_j and $\bar{H}_j$ represent the absorbed heats from a monoenergetic source with gamma energy E, and $S_j(E)$ is the relative intensity of the j th spectral group in the gamma energy spectrum.

2.2 Discussion

Errors in the absolute determination of the total heat absorbed per unit length of the peak rod could result from errors, uncertainties or approximations in the following:

(a) The analytical model employed in the solution of the Boltzmann gamma transport equation,

(b) The gamma ray attenuation and energy deposition coefficients,

(c) The selected core volume size beyond which all gamma sources can be neglected,

(d) The geometric representation of this core volume by a matrix suitable for use with the shielding code employed,

(e) The representation of volumetric sources by discrete source points,

(f) The representation of unit length of the peak rod by a set of point detectors,

(g) The evaluation of gamma source intensities and spectra in the fuel clad, coolant and structural material as compared to those in the fuel, and

(h) The non-uniform source distributions within the fuel rods.

It is evident therefore that evaluation of H_γ on an absolute basis with an error of only a few percent is extremely difficult. And when the redistribution factor is determined by Eq. (6) then any error in H_γ will be carried over to F_γ. When however, the gamma redistribution factor is determined by the relative approach (that is Eq. 10 or 11), then the errors in H_γ and $\bar{H}_\gamma$ will tend to cancel out and the uncertainty in F_γ will be sub tantially reduced.

This then is the main advantage of the technique used in this work over that requiring the absolute determination of the absorbed heat. A few additional benefits of the method are described below.

It would appear at first glance that the parameter n in Eq. (11) should be large so that the summations represent the total heats absorbed as accurately as possible. Actually, an accurate, conservative value for F_γ can be obtained by considering only a small number of rods in the analysis. From the mathematical point of view, as shown later, a conservative (i.e., close to unity) F_γ value would result if one excludes from the summations all rods satisfying the condition

$$\frac{k_j \, h_j}{\bar{h}_j} < F_\gamma \tag{13}$$

where F_γ is now assumed to be a predetermined quantity, that is, already computed using other rods closer to the peak rod. The same would also apply for a group of rods beyond those already considered, the inequality now taking the form

$$\frac{\sum_{j=1}^{\ell} \frac{k_j \, h_j}{\bar{h}_j}}{\sum_{j=1}^{\ell} \bar{h}_j} < F_\gamma \, . \tag{14}$$

If the rods in this group are approximately the same distance from the peak rod, Eq. (14) can be approximated by

$$\bar{\bar{k}} < F_\gamma \tag{15}$$

where $\bar{k}$ is the average relative peaking factor given by

$$\bar{k} = \frac{1}{\ell} \sum_{j=1}^{\ell} k_j \quad (16)$$

These equations were obtained by considering two redistribution factors defined as

$$F_1 = \frac{A}{B} \quad (17)$$

and

$$F_2 = F_1 + \Delta F = \frac{A + \Delta A}{B + \Delta B} \quad (18)$$

where ΔA and ΔB are changes brought about by the inclusion of one or more rods. It then follows that

$$\Delta F = \frac{B\Delta A - A\Delta B}{B\,(B + \Delta B)} \quad (19)$$

and this parameter will be negative whenever

$$A\Delta B \rangle A \quad (20)$$

or, in a form similar to Eqs. (13) and (14),

$$\frac{\Delta A}{\Delta B} \langle F_1 \quad (21)$$

Thus, if one neglects ΔA and ΔB in the analysis, that is, if one considers fewer rods, the redistribution factor would change from F_2 to F_1 and F_1 will be larger than F_2 (i.e., a conservative move) if Eq. (21) is satisfied. ΔF is positive if the fractional change in A is greater than that in B, that is,

$$\Delta F \rangle 0 \quad \text{if} \quad \frac{\Delta A}{A} \rangle \frac{\Delta B}{B} . \quad (22)$$

Note that the inequality represented by Eq. (14) can be readily satisfied since some k_j values are equal to zero. Thus, whereas only a small

number of rods is needed for the evaluation of the redistribution factor by the approach used in this work, an absolute determination of H_γ in Eq. (6) with reasonable accuracy requires the inclusion of all rods within at least 4 or 5 mean free paths of the most penetrating gamma rays in the source spectra.

Another advantage of the method is the insensitivity of the model on the coolant density. To understand this let F_1 and F_2 in Eqs. (17) and (18) be the results obtained using two different coolant densities. F_1 is for the high coolant density and F_2 is for the low density. ΔA and ΔB then represent the increases in the heat absorbed by the peak rod due to the decreased gamma ray absorption by the coolant, and since the heat absorbed by the coolant is directly proportional to the heat generated in the fuel rods it follows that $(\Delta A/A)$ is approximately equal to $(\Delta B/B)$ and, therefore, from Eq. (19) ΔF is approximately equal to zero. In addition, as can be concluded by comparing Eqs. (9) and (10), redistribution factors computed by the model described in this report correspond to the case of zero coolant density in a model which involves the absolute determination of absorbed heat.

From the analysis and reasoning discussed above, it is clear that the model is equally insensitive to secondary sources of gamma radiation which are present in both the uniform and actual core configurations. Note that the intensities of these sources, such as activation products in the cladding and coolant, would be higher in the uniform array case with uniform power (equal to that of the peak rod) than in the corresponding actual geometry and power distribution.

2.3 Equations for Absorbed Heat

The parameters $\bar{h}_i$ and h_i in Eq. (11) for the gamma redistribution factors represent the heats absorbed per unit length of the peak rod from gamma rays emanating from rod i. The peak rod is identified by i = 1, and h_1 (equal to $\bar{h}_1$) is the energy deposition from gamma rays originating within the peak rod itself (i.e., self-heating). In this work, h_1 was determined from the expression (Ref. 4)

$$h_1 = \frac{\pi R^2 C E \mu_a S_v}{\mu} \sum_{m=o}^{3} m!\ a_m\ \bar{\psi}_m\ (\mu R) \qquad (23)$$

where

h_1 = peak rod self-heating (cross-rod average) (W/cm)

R = rod radius (cm)

C = 1.602×10^{-13} (W - sec/MeV)

E = initial gamma energy (MeV)

μ_a = energy deposition coefficient at energy E (also known as the linear energy absorption coefficient) (cm^{-1})

μ = total linear attenuation coefficient at energy E (cm^{-1})

S_v = volumetric source intensity (assumed uniform) photons/cm^3 - sec)

a_m = buildup - factor coefficients:

$$(B = \sum_{m=o}^{3} a_m (\mu R)^m, \quad B = \text{buildup factor})$$

$\bar{\psi}_m$ = averaged collision probabilities.

Closed form analytical expressions for the $\bar{\psi}$ functions are available only for $\bar{\psi}_o$ and $\bar{\psi}_1$. $\bar{\psi}_2$ and $\bar{\psi}_3$ on the other hand can be either computed by

numerical integration or extracted from a graphical presentation of these functions in the literature (see Fig. 2.3.1). The expressions for $\bar{\psi}_o$ and $\bar{\psi}_1$ are:

$$\bar{\psi}_o = 1 - \frac{2\mu R}{3}\left\{ 2\mu R \left[K_1 I_1 + K_o I_o\right] - 2 + \frac{1}{\mu R}\left[K_1 I_1\right] - K_o I_1 + K_1 I_o\right\} \quad (24)$$

and

$$\bar{\psi}_1 = 1 - 2 I_1 K_1 \quad (25)$$

where $I_n(x)$ and $K_n(x)$ are the modified Bessel functions of first and second kind, respectively, evaluated at $x = \mu R$.

The energy deposition rate in the peak rod from gamma rays originating in surrounding rods was calculated using the computer code SHADRAC (Ref. 5). This is a General Dynamics code that computes neutron and/or gamma spectra, direct-beam flux, heat generation rate, and/or dose rate received at a point detector from a source of radiation. The program is the culmination of shield-penetration studies based on the moments-method solution of the neutron and gamma-ray transport equation. The model is based on the differential energy spectra for a point isotropic source in an infinite medium along with appropriate edge correction factors to describe radiation transport in finite media. In addition, the assumption is made that the only portion of a system of radiation sources, shields and detectors which affects dose rate (or spectra and heat-generation rate) is that part of the system on the line of sight between the source and the detector.

The moments-method data used in SHADRAC is for point isotropic sources. Therefore, distributed sources in any given geometric configuration must be approximated by a set of point sources. Each of these point

sources must represent the radiation generated in an elemental volume containing the point such that an integration of the source points over the source volume will equal the total radiation generated by the distributed source. Similarly, a number of detector points must be utilized to compute the total heat generation rate (or average dose rate) in an absorber of finite dimensions.

A major limitation of the program is its restriction to geometries composed of frusta of rectangular pyramids and coaxial cylinders. The explicit representation of a reactor core section is therefore possible only if one assumes that the fuel rods have a rectangular (in fact, square) cross-section. Also, because of the point-to-point kernels used, and the inverse square law in the transport of gamma radiation, the code cannot be used for reliable self-heating calculations. It is this latter limitation that prompted the use of Eq. (23) above.

2.4 Error Equation

To obtain an estimate of the error in the gamma redistribution factor as defined by Eq. (11) it is important to modify the said expression to reflect the fact that some of the h_i and $\bar{h}_i$ are identical and that the only difference between these two parameters results from differences in the attenuating properties of the material between sources and detectors. Thus, without any approximation, one can define

$$h_i = b_i \bar{h}_i \tag{26}$$

where b_i represents a gamma-ray relative attenuation correction factor. Recall that the barred symbol represents the uniform array of rods with uniform source intensity.

When Eq. (26) is substituted into Eq. (11) one obtains

$$F_\gamma = \frac{H_\gamma}{\bar{H}_\gamma} = \frac{\sum_i k_i b_i \bar{h}_i}{\sum_i \bar{h}_i} \qquad (27)$$

This modification from Eq. (11) to Eq. (27) is important since the error in F_γ may be over-estimated if one considers h_i and $\bar{h}_i$ as two completely independent parameters.

To proceed further, since b_i is a function only of the fairly well known attenuating properties of the materials between a source and a detector in the actual core configuration as compared to the uniform array of rods, the error in b_i may be neglected in comparison to that in $\bar{h}_i$. In addition, even though the error in the absolute peaking factors could be significant, the error in the relative peaking factor k_i is also negligible, particularly when one considers only a very small fraction of the core. With these assumptions then, and according to the equation for the propagation of errors, the equation for the square of the error in F_γ is simply

$$\sigma^2(F_\gamma) = \sum_i \left[\frac{\partial F_\gamma}{\partial \bar{h}_i}\right]^2 \sigma^2(\bar{h}_i) \qquad (28)$$

where $\sigma(\bar{h}_i)$ is the error in $\bar{h}_i$. From Eq. (27) one also has

$$\frac{\partial F_\gamma}{\partial \bar{h}_i} = \frac{\bar{H}_\gamma k_i b_i - H_\gamma}{\bar{H}_\gamma^2} = \frac{k_i b_i - F_\gamma}{\bar{H}_\gamma} \qquad (29)$$

and therefore

$$\sigma^2(F_\gamma) = \sum_i \left[\frac{k_i b_i - F_\gamma}{\bar{H}_\gamma}\right]^2 \sigma^2(\bar{h}_i) \qquad (30)$$

Expressed differently,

$$E^2(F_\gamma) = \frac{1}{F_\gamma^2} \sum_i \left[\frac{k_i b_i - F_\gamma}{\bar{H}_\gamma} \cdot \bar{h}_i \right]^2 E^2(\bar{h}_i) \qquad (31)$$

where

$$E(F_\gamma) = \sigma(F_\gamma)/F_\gamma \qquad (32)$$

$$E(\bar{h}_i) = \sigma(\bar{h}_i)/\bar{h}_i \qquad (33)$$

and represent the fractional errors in the two parameters.

Since $E(\bar{h}_i)$ is not a readily determinable quantity, it was necessary to assume that the error in each $\bar{h}_i$ is approximately the same, that is,

$$E(\bar{h}_i) = c \qquad (34)$$

where c is a constant. The basis for this assumption is that all $\bar{h}_i$ are computed using the same analytical procedure and data. Moreover, since

$$\bar{H}_\gamma = \sum_i \bar{h}_i \qquad (35)$$

and

$$\sigma^2(\bar{H}_\gamma) = \sum_i \sigma^2(\bar{h}_i) = c^2 \sum_i (\bar{h}_i)^2 \qquad (36)$$

it follows that

$$c^2 = \frac{\sigma^2(\bar{H}_\gamma)}{\sum_i (\bar{h}_i)^2} \qquad (37)$$

and therefore

$$E(F_\gamma) = \mathbb{Z}\, E(\bar{H}_\gamma) \qquad (38)$$

where E $(\bar{H}_\ell)$ is the fractional error in $\bar{H}_\gamma$ and

$$Z^2 = \frac{1}{F_\gamma^2 \sum_i (\bar{h}_i)^2} \sum_i \left[\left(k_i \, b_{\perp} \quad r_\gamma \right) \bar{h}_i \right]^2 \tag{39}$$

Note that Z can be computed without any difficulty since all the parameters in Eq. (39) are known. Therefore, according to Eq. (38), only the error in $\bar{H}_\gamma$ is needed for the determination of E (F_γ). And an estimate of the error in $\bar{H}_\gamma$ can be obtained from Eq. (8) when one compares the calculated total heat absorbed per unit length of a rod-coolant cell to the actual heat assumed(in the form of input data) to be generated per unit length of the peak rod.

Finally, using Eq. (5) and the equation for propagation of errors, the fractional error is the redistribution factor is equal to

$$E(F) = \gamma E(F_\gamma) \tag{40}$$

The equation is based on the assumption that the error in γ is negligible.

2.5 Rule-of-Thumb Approach

Evaluation of the gamma redistribution factor by the method described above is a long, tedious and complex process. It is possible, however, to obtain a reasonable estimate of this factor by using only the rod peaking factors.

To understand this rule of thumb consider a set of rods immersed in a coolant. The decay heat generated by rod j is equal to $G_\gamma \, k_j$ where, as defined earlier, G_γ is the heat generated by the peak rod and k_j is the relative peaking factor. Similarly, the decay heat absorbed by rod j

and the coolant cell around it can be represented by $(H_\gamma+H_c)k_j^*$ where $(H_\gamma+H_c)$ is the heat absorbed by the peak rod and its coolant and k_j^* is hereby defined as a relative heat absorption factor. In essence, the parameters k_j and k_j^* represent the gamma source and the gamma heating distributions, respectively. If the system is assumed to be free of structural material, the total heats generated and absorbed by a small number of rods at the center of the system are approximately equal, that is,

$$G_\gamma \sum_{j=1}^{n} k_j = (H_\gamma+H_c) \sum_{j=1}^{n} k_j^* \quad . \tag{41}$$

Therefore, according to Eq. (6),

$$F_\gamma = \frac{\bar{k}}{\bar{k}^*} - \frac{H_c}{G_\gamma} \tag{42}$$

where

$$\bar{k} = \frac{1}{n} \sum_{j=1}^{n} k_j \tag{43}$$

and

$$k^* = \frac{1}{n} \sum_{j=1}^{n} k_j^* \tag{44}$$

Note that $\bar{k}$ and $\bar{k}^*$ are less than unity and that $\bar{k}^*$ is larger than $\bar{k}$ due to the flattening of the heating source by the gamma smearing effect. A flat heating distribution corresponds to $\bar{k}^* = 1$, a condition physically achievable with zero-coolant density and high energy gamma photons. For this particular case Eq. (42) reduces to the simple form

$$F_\gamma = \bar{k} \quad . \tag{45}$$

The results presented in Sec. 4 indicate that this equation is satisfied at gamma energies greater than about 2 MeV. To a good approximation, however, the equation may be considered applicable at any energy. But note that, in view of the low-energy gamma photons in the actual decay spectrum, redistribution factors obtained by Eq. (45) tend to be underestimated. In general, Eq. (45) provides a good rule of thumb. It is important however that the equation be applied to a uniform array of fuel rods and that the control blade be properly represented by a set of rods with zero power.

3.0 CORE REPRESENTATION AND SOURCE TERMS

3.1 Fuel Rod

The mechanical design parameters of Yankee Rowe Core XI fuel rods are similar to the Zircaloy-clad rods in Core X. They are as follows (Ref. 6):

Fuel material	UO_2
Pellet diameter, inches	0.3105
Pellet dish depth, inches	0.006 to 0.0135
Pellet dish diameter, inches	0.242
Pellet length, inches	0.5 to 0.7
Pellet density (% theoretical)	94.5
Effective pellet density, g/cc	10.36
Clad material	Zircaloy -4
Clad material density, g/cc	6.55
Clad I.D., inches	0.317
Clad O.D., inches (nominal)	0.365
Clad thickness, inches	0.024
Active length, inches	91.0

Based on the reasoning discussed in Sec. 2.2, it was possible to convert the Zircaloy clad into an equivalent thickness of UO_2 and to represent a fuel rod by an effective radius R equal to

$$R = \frac{0.3105}{2} + \frac{0.024 \times 6.55}{10.36}$$

$$= 0.1704 \text{ inches}$$

$$= 0.433 \text{ cm}$$

This value was used in Eq. (23) for the evaluation of h_1. Determination of the other h_1 parameters, on the other hand, using SHADRAC, required the conversion of the circularly cylindrical fuel rods into parallelepipeds with square cross-section. To account for all the UO_2 material in a rod, the cross-sectional area of the equivalent parallelepiped was set equal to πR^2 (i.e. 0.589 cm^2). In addition, since the code is based on the use of point-to-point kernels, it was necessary to subdivide the fuel rod cross-sectional area into a number of equal segments and to represent each segment by a point. As shown in Fig. 3.1.1, a total of 12 segments were used in the subdivision. The centroids of these segments were determined analytically in terms of the effective radius R. The equations appear in Fig. 3.1.1.

The centroids in Fig. 3.1.1 were selected to represent a set of detector points in the peak rod. A similar arrangement was also used at the start of this work to represent a set of line sources in the peak rod for the determination of h_1, the self-heating contribution. Eventually h_1 was determined (more accurately) by Eq. (23).

Representation of the gamma activity in the remaining fuel rods was by a maximum of 4 line sources in each rod near the peak rod and by a single line source in the distant rods. (The source arrangement appears in Fig. 3.2.3).

3.2 Lattice

The core section of interest is shown in Figs. 3.2.1 and 3.2.2. It consists of a control blade and a total of 100 fuel rods immersed in coolant. The control blade, which consists of a mixture of Ag, In and Cd, has an average density of 9.67 g/cm^3. The coolant was assumed to have a density of 1 g/cm^3. All other structural material was neglected.

Since SHADRAC permits the use of a maximum of 64 regions, it was necessary to subdivide the core section in Fig. 3.2.2 into 4 quadrants. Each quadrant was then analyzed separately and the results were then combined with a computer program specially written for this purpose.

The geometrical arrangement in Fig. 3.2.3 was used to represent each of these quadrants. To make this possible it was necessary to assume that the assemblies are physically closer to each other, that the fuel rods are located at the nodes of a uniform grid and that the thickness of the control blade is slightly less (about 7 percent) than actual and equal to that of the parallelepiped representing the fuel rod. Also, all other structural material was neglected. These assumptions are all conservative since they result in increased heat absorption by the peak rod.

The uniform array configuration for evaluation of $\overline{H}_\gamma$ in Eq. (10) was obtained by combining 4 quadrants similar to quadrant A in Fig. 3.2.2.

The fuel rods in Fig. 3.2.3 were assigned into six source groups according to their distance from the peak rod as follows: source group 1 for the peak rod, group 2 for all rods next to the peak rod, group 3 for rods next to and surrounding group 2, etc. With this grouping, it was possible, as shown in Sec. 4.2, to obtain by graphical extrapolation an estimate of the heat absorbed by the peak rod from gamma rays emanating from rods further away than those in group 6.

The numbers in Fig. 3.2.2 are the radial peaking factors for the beginning of life of Core XI (Ref. 7). Division of these numbers by 1.773, the largest peaking factor, yields data for the k_i parameters in Eq. (11). Additional data pertaining to group peaking factors and

the application of Eq. (15) appears in Table 3.2.1. In this table, ℓ is the total number of rods per source group in the uniform array configuration (4 quadrants). The group 2 entry is low because five of the eight k_j values represent part of the control blade and are equal to zero. Data for $\bar{k}$ in Eq. (43) for combined groups is given in Table 3.2.2.

In Figs. 3.2.2 and 3.2.3 the third dimension ranges from x = - 115.6 to x = 115.6 cm. This is equivalent to the 91-inch active length of the fuel rods.

TABLE 3.2.1

Relative Peaking Factors - Source-Group Averages

GROUP	ℓ	$\bar{\bar{k}}$
1	1	1.000
2	8	0.327
3	16	0.630
4	24	0.664
5	32	0.674
6	40	0.670
7	48	0.663
8	56	0.644
9	64	0.646

$\bar{\bar{k}}$ is defined by Eq. (16).

TABLE 3.2.2

Relative Peaking Factors - Combined Source-Group Averages

GROUPS	n	$\bar{k}$
1	1	1.000
1, 2	9	0.402
1-3	25	0.548
1-4	49	0.605
1-5	81	0.632
1-6	121	0.645
1-7	169	0.650
1-8	225	0.648
1-9	289	0.649

$\bar{k}$ is defined by Eq. (43)

3.3 Source Activities

Since the SHADRAC code is based on the use of point-to-point kernels, it was necessary to represent each of the line sources in Fig. 3.2.3 by a set of point sources along the x axis. The source intensitites were therefore expressed in terms of unit source lengths and the h_i parameters in Eq. (11) were computed by subjecting the SHADRAC results to numerical integration along this axis.

To permit evaluation of the functional dependence of the redistribution factor on gamma energy, the analysis was repeated a number of times using monoenergetic sources. The point source intensities were selected arbitrarily. The selection, however, was such that the relative heat generation rate in a rod was the same at all energies. Subsequent conversion of the assumed intensities to actual heat yielded 0.04545 W/cm. Based on this number, the volumetric source intensity S_v in Eq. (23) takes on the following values:

E_j (MeV)	S_v (photons/cm^3 - sec)
0.5	9.633×10^{11}
1.0	4.816×10^{11}
1.38	3.490×10^{11}
2.0	2.408×10^{11}
3.0	1.605×10^{11}

and is given by

$$(S_v)_j = \frac{0.04545}{\pi R^2 C E_j} \qquad (46)$$

The parameters in this equation were defined in Sec. 2.3.

The source intensity data in rod i at energy E_j required as input to SHADRAC is given by

$$P_{ij} = \frac{(S_v)_j A_i k_i \ell_i}{\Delta E_j} \text{ photons/(sec - cm - MeV)} \qquad (47)$$

where A_i is the segmented area (in cm^2) of a rod represented by the point source, ΔE_j is the energy bin width (in MeV) as specified in SHADRAC, and g is a geometric factor equal to 0.5 for source points common to neighboring quadrants and equal to 1 otherwise. For the E_j data in the above table, ΔE_j is equal to 0.25, 0.25, 0.25, 0.375, 1.0 and 1.0 MeV, respectively.

The numerical integration along the axis was between x = - 10 and x = 10 cm.* Since this represents only a small fraction of the fuel rod active length, the variation of source intensities along this axis according to the cosine law was neglected. This is a conservative assumption since it leads to an increase in the heat absorbed by the peak rod in the actual core geometry and power distribution (i.e., in H_γ in Eq. (10)).

Gamma rays from activation products in the coolant were not considered. As pointed out in Section 2.2 the model employed in this work is insensitive to secondary sources of gamma radiation which are present in both the uniform array and actual core configurations. The activity of the control blade was also neglected since it was estimated to be insignificant compared to that of the fuel rods. As shown in Figure 3.2.1, this control blade is used only for shutdown purposes and is withdrawn from the core during normal operation. The blade was assumed to become fully inserted at the time of the accident. Note that the Yankee Rowe control blades have Zircaloy followers.

---

*As discussed later in Section 4.2, this limit of integration undervalues the heating rate in the uniform array case by a maximum of 6 percent for the most penetrating gamma rays.

4.0 RESULTS

4.1 Peak Rod Self-Heating

Data for the parameters in Eq. (23) appear in Table 4.1.1. The buildup factor coefficients a_m were computed using the expression

$$a_m = \sum_{k=o}^{4} C_{mk} \quad /E)^k \tag{48}$$

and the C_{mk} data for uranium in Reference (4). The data for μ and μ_a is identical to that in SHADRAC. The results obtained for h_1, the self-heating contribution, are as follows:

E_j (MeV)	h_1 (W/cm)
0.5	0.0208
1.0	0.00969
1.38	0.00765
2	0.00700
3	0.00729

Recall that the peak rod was assumed to generate 0.04545 W/cm at each gamma energy. At 0.5 MeV, approximately 46 percent (i.e. 0.0208/0.04545) of this heat is absorbed by the peak rod itself. At 1 MeV the fraction drops to 21 percent and at about 2 MeV it reaches a minimum of approximately 15 percent.

TABLE 4.1.1

Data for the evaluation of h_1

E (MeV)	μ_a (cm^2/g)	μ(cm^2/g)	μR	I_o	I_1	K_o	K_1	S *
0.5	0.132	0.176	0.789	1.162	0.4256	0.5749	0.8801	9.613
1.0	0.0482	0.0757	0.340	1.029	0.1725	1.259	2.647	4.816
1.38	0.0363	0.0580	0.260	1.017	0.1311	1.505	3.588	3.490
2	0.0324	0.0484	0.217	1.012	0.1092	1.675	4.376	2.408
3	0.0332	0.0445	0.200	1.010	0.1005	1.753	4.776	1.605

E (MeV)	a_o	a_1	a_2	a_3	$\bar{\Psi}_o$	$\bar{\Psi}_1$	$\bar{\Psi}_2$	$\bar{\Psi}_3$
0.5	1.00170	0.3262	-0.004659	0.0002041	0.5277	0.2509	0.11	0.047
1.0	1.00613	0.2649	-0.01224	0.0003731	0.3107	0.08680	0.023	0.013
1.38	1.00841	0.2232	-0.01360	0.0004359	0.2544	0.05923	0.015	0.008
2	1.01073	0.1790	-0.01431	0.0004877	0.2201	0.04428	0.011	0.005
3	1.01275	0.1396	-0.01456	0.0005251	0.2070	0.04002	0.010	0.004

*$S_v = 10^{11}$ photons/cm^3 - sec

4.2 Heat from Neighboring Rods

In Fig. 4.2.1 are presented typical hot spot heating rate distributions as functions of gamma enegy and source x-plane elevation. The curves were obtained by combining the SHADRAC results for the four quadrants and 12 detectors and by moving the yz plane containing the sources in Fig. 3.2.3 along the x-axis. The distributions in Fig. 4.2.1 are for the uniform array/source intensity case and include a total of 120 rods around the peak rod.

The hot spot heating rate (in W/cm) due to gamma rays of energy E_j emanating from all neighboring rods is equal to

$$2 \left(\pi R^2/12 \right) I = 0.0\overline{9}12 I \qquad (49)$$

where the 2 multiplier accounts for negative x values, $(\pi R^2/12)$ is the segmented area of the peak rod representing a point detector, and I is the integral of curves similar to those in Fig. 4.2.1. The results obtained are as follows:

E_j (MeV)	$\sum_{i=2}^{n} \bar{h}_i$	$\sum_{i=2}^{n} k_i h_i$
0.5	.0193	.00953
1.0	.0254	.0138
1.38	.0247	.0136
2	.0246	.0135
3	.0246	.0132

Note that each entry in this table represents the evaluation of approximately 10,000 point-to-point kernels.

The I integrals were obtained by fitting n-degree polynomials to the data points and performing a parabolic-rule integration using interpolated and extrapolated data. The polynomial was cubic from $x = 0$ to $x = 6$ cm and quadratic for $x > 6$. In this work, the limit of integration was set equal to $x = 10$ cm. It was estimated that choice of this limit undervalues the heating rate in the uniform array case by a maximum of about 6 percent. In terms of the gamma energies used in the analysis the following results were obtained for I/I_∞, the ratio of the integral I as defined above and a similar integral covering the entire range:

E_j (MeV)	I/I_∞ (estimated)
0.5	1.0
1	0.98
1.38	0.96
2	0.94
3	0.94

With regard to the effect of the number of fuel rods used, the 121 rod configuration in the uniform array/source intensity case was estimated to undervalue the heating rates by the following fractions:

E_j (MeV)	Fraction (estimated)
0.5	1.00
1	0.94
1.38	0.89
2	0.84
3	0.81

These estimates were obtained with the use of Fig. 4.2.2 where the hot spot heating rate is presented in terms of the source groups identified

in Fig. 3.2.3. The data points in Fig. 4.2.2 were computed using Eq. (49) and a 0 to 10 cm integration for the integral I. Note that the points can be fitted approximately by a simple exponential curve at each energy. The slopes of these curves were found to be directly related to the linear attenuation coefficient μ. In fact, the estimated fractions in the last table are equal to $(1 - \exp(-\mu t))$ where $t = 37.8$ g/cm^2 and represents the product of the average density of the region used in the analysis (about 5.2 g/cm^3) times an effective attenuation distance of 7.27 cm.

It is clear from the above that at low energies all sources located outside the region used in the evaluation of $\bar{H}_\gamma$ contribute insignificantly to this parameter. At high energies on the other hand, due to the longer mean free paths of the gamma photons, a substantial amount of the absorbed heat comes from sources beyond the region described. Thus, at 3 MeV, for instance, if one wishes to account for 99 percent of the sources, one must analyze a region with an equivalent spherical radius of approximately 20cm. A region of this size would contain about 900 fuel rods.

4.3 Gamma Redistribution Factors for Monoenergetic Sources

The total heat absorbed per unit length of the peak rod at various gamma energies is equal to the sum of the data in the previous sections. The results are presented in the table below along with data for the gamma redistribution factor for monoenergetic sources.

E_j (MeV)	$\bar{H}_\gamma$ (W/cm)	H_γ (W/cm)	F_γ (monoenergetic)
0.5	0.0401	0.0303	0.756
1	0.0351	0.0235	0.670
1.38	0.0324	0.0213	0.657
2	0.0316	0.0205	0.649
3	0.0319	0.0205	0.643

A graphical presentation of this data is shown in Fig. 4.3.1. Note that by extrapolating the results to lower gamma energies, the two curves merge together at E = 0 MeV and that at this point the absorbed heat is equal to the heat assumed (in the form of input data) to be generated by the peak rod. This result can serve as a measure of the overall accuracy of the procedure, computer codes, computations and data used in this work.

Gamma redistribution factors were also computed using only few of the source groups in Fig. 3.2.3. The results obtained at E = 1 MeV are as follows:

Source Groups	$\bar{H}_\gamma$ (W/cm)	H_γ (W/cm)	F_γ (monoenergetic)
1	0.00969	0.00969	1.000
1,2	0.0204	0.0135	0.662
1-3	0.0271	0.0178	0.657
1-4	0.0309	0.0205	0.663
1-5	0.0334	0.0223	0.668
1-6	0.0348	0.0234	0.672
1-7			<0.672

The data in the 6th row corresponds to the 1 MeV entry in the previous table, the small difference between the two sets being attributable to the errors incurred in the evaluation of the integrals I. The entry in the last row was obtained through the use of Eq. (15) by comparing the F_γ values above with the $\bar{k}$ data in Table 3.2.1. Note that a reasonable estimate of F_γ could have been arrived at by using only 3 or 4 source groups.

4.4 Peak Rod Redistribution Factor

In Fig. 4.4.1 are shown plots of F, F_γ and $_\gamma$ as functions of time after shutdown. The curves for the redistribution factors are spectrum - weighted averages based on Eqs. (5) and (12) and on the results for monoenergetic sources in Sec. 4.3. Data for the gamma contribution to the decay heat and for the decay gamma spectra was extracted from Refs. (3) and (8).

It is seen from Fig. 4.4.1 that the peak rod redistribution factor F decreases monotonically from a value of approximately 0.845 at time zero to 0.820 at 1000 seconds after shutdown. This variation is mainly due to the increase with time of the decay heat gamma fraction. The weighted gamma redistribution factor F_γ, on the other hand, increases but only slightly, with time. This increase is due to the softening of the gamma spectrum with time. The average value obtained for this parameter is approximately equal to that for a monoenergetic source with 1 MeV gamma photons.

Note that the results presented in Fig. 4.4.1 are for the peak rod identified in Fig. 3.2.2. In addition, in view of the relative approach used in the analysis, the results apply at any position along the axis of this rod. This is because the variation of power along the x-axis in Fig. 3.2.3 is the same for all rods and therefore the relative peaking factors are independent of the elevation of the yz plane.

4.5 Error Estimates

An estimate of the error in $\overline{H}_\gamma$, the absorbed heat in the uniform array uniform intensity case, was obtained by comparing the calculated total heat absorbed per unit length of a rod-coolant cell to the actual heat assumed to be generated per unit length of the peak rod. The analysis was carried out using the 0.5 MeV results since at this energy all gamma sources located outside the region used in the evaluation of $\overline{H}_\gamma$ were found to contribute insignificantly to this parameter. The heat absorbed per unit length of a coolant cell surrounding the peak rod was also computed using SHADRAC and a model similar to that for the peak rod. A summary of the results on which evaluation of the error in the absorbed heat was based is as follows (in W/cm):

Assumed heat generation rate	0.04545
Heat absorbed by peak rod ($\overline{H}_\gamma$)	0.0401
Heat absorbed by coolant cell	0.001
Total heat absorbed by rod/coolant	0.0411
Generated heat not-accounted for	0.00435

The last entry provides a direct measure, on an absolute basis, of the error in $\overline{H}_\gamma$. It is non-zero mainly because of the representation of the fuel rod activities by a finite number of point sources and can therefore apply at all energies.

Based on the above information and on Eqs. (33) and (40) the fractional errors in the various parameters are as follows:

$$E\ (\overline{H}_\gamma) = 0.11$$

$$E\ (F_\gamma) = 0.048$$

$$E\ (F) = 0.023$$

A conservative value of 0.482 was used for γ in Eq. (40) and, therefore, the errors can be assumed to apply at any time after reactor shutdown.

4.6 Rule-of-Thumb Results

In the previous sections attention was confined to the peak rod and its redistribution factor. What is of interest now is to determine whether some other rod, whose heat absorption rate during shutdown is affected only slightly by the gamma smearing effect, could become the controlling rod in a LOCA. In other words, it is important to verify that the rod with the peak power during normal reactor operation is also the rod with the peak heat absorption rate following shutdown.

This question was answered by applying the rule-of-thumb model described in Sec. 2.5. In particular, redistribution factors were first

computed for a number of rods around the peak rod by making use of Eqs. (5), (43) and (45). The results were then multiplied by the corresponding actual peaking factors to obtain and compare the relative heat absorption rates by the various rods.

Gamma redistribution factors computed as described are shown in Fig. 4.6.1. These were based on the use of 121 relative peaking factors around the rod of interest. In each case, 21 relative peaking factors were equal to zero and represented the control blade. Note that the peak rod gamma redistribution factor is the smallest and corresponds to the 6-group entry in Table 3.2.2. This table may be referred to for additional results based on the use of smaller and larger numbers of relative peaking factors. The rod which experiences the next highest gamma smearing effect is diagonally across the control blade relative to the peak rod.

The peak rod gamma redistribution factor determined by this crude model compares very favorably with the results in Sec. 4.3 for the 2 and 3-MeV gamma photons. Indeed, it is this approximate equality of the results by the two models that has justified and encouraged the use of the rule-of-thumb approach.

Also shown in Fig. 4.6.1 are the redistribution factors F for zero decay time following shutdown (i.e., $\gamma = 0.482$). This data was used in conjunction with the actual peaking factors to compute the relative heat absorption rates in the various rods. The results, which are equal to the products of these two parameters, are shown in Fig. 4.6.2. The peaking factors during normal reactor operation are also given for direct comparison. A plot of the quadrant-A peaking factors before and after redistribution appears in Fig. 4.6.3. Note that the peak rod is controlling also during shutdown, a result that we set out to prove.

5.0 SUMMARY AND CONCLUSIONS

This study has shown that, due to the gamma smearing effect, the decay heat absorbed by the peak rod in Core XI of Yankee Rowe is substantially less than the decay heat it produces. A summary of the results, presented in terms of the redistribution factor F (i.e., the ratio of the decay heat absorbed per unit length of the peak rod to that generated per unit length) and the decay time t after shutdown, is as follows:

F(t = 0 sec.)	=	0.845
F(t = 10 sec.)	=	0.829
F(t = 100 sec.)	=	0.820
F(t = 1000 sec.)	=	0.820

As explained in the main body of this report, these results were obtained through the use of a number of conservative assumptions. Smaller, less conservative numbers would have been obtained if more fuel rods were used in the analysis, if the control blade was not assumed to be thinner than it actually is, or if the axial cosine power distribution was taken into account. Additional conservatism, on the other hand, can be obtained by increasing the above results to include the maximum value of the error estimate. In this case, since the error in the analysis was determined (on an absolute basis) to be approximately 2.3 percent, the redistribution factor takes on the following values:

F(t = 0 sec.)	=	0.864
F(t = 10 sec.)	=	0.848
F(t = 100 sec.)	=	0.839
F(t = 1000 sec.)	=	0.839

It is of interest to note that the redistribution factors given above compare very favorably with the ratio of certain nuclear heat flux factors computed by Westinghouse and reported in the original Yankee Rowe FHSR. Specifically, the following entry appears in the FHSR section dealing with the loss-of-coolant accident (Ref. 2):

> "F_Q^N (the nuclear heat flux factor) is 3.88 for steady state conditions and 3.23 for decay heat calculations."

The ratio of these two numbers, i.e., 3.23/3.88, is the redistribution factor as defined in this work and is equal to 0.832. Unfortunately, since these results were obtained more than 13 years ago, it was not possible to obtain specific details on the analytical model and assumptions employed in that work.

Finally it was shown in this report that reasonably accurate redistribution factors can be obtained through the use of a very simple formula. This formula, which involves only 100 to 150 relative peaking factors around the peak rod, was used in this work to verify that the peak power rod during normal reactor operation is also the rod with the highest heat absorption rate during reactor shutdown.

REFERENCES

1. AEC Regulatory Staff Testimony, "Interim Acceptance Criteria for Emergency Core Cooling Systems for Light-Water Power Reactors", AEC Docket No. RM-50-1, (Sec. 3.2.4.5) January 27, 1972.

2. Yankee Nuclear Power Station, Rowe, Massachusetts, Final Hazards Summary Report, AEC Docket No. 50-29, (p. 402.21, 3/31/61).

3. G. J. Scatena, G. L. Upham, "Power Generation in a BWR following Normal Shutdown or Loss-of-Coolant Accident Conditions", NEDO-10625, March, 1973.

4. R. G. Jaeger, Editor, "Engineering Compendium on Radiation Shielding", Vol. I, pp 212-219, 443-446, Springer-Verlag, New York, 1968.

5. "SHADRAC, Shield Heating and Dose Rate Attenuation Calculation", General Dynamics, GE-1365, March, 1966.

6. P. Buck, J. Fiscella, P. Lemberg, "Nuclear Design and Analysis of Yankee Rowe Core 10", United Nuclear Corp., Report No. UNC-5275, p. 27, June, 1971.

7. R. J. Cacciapouti, "Nuclear Analysis of Yankee Core XI", Yankee Atomic Electric Company, Report No. YAEC-1072, June 1974 (PDQ 7 Run No. VNA-Y-648, 10/02/73).

8. Combustion Engineering, Amendment No. 1 to CENPD-16

Fig. 2.3.1 The functions for calculating the average gamma heating in cylinders (from Ref. 4)

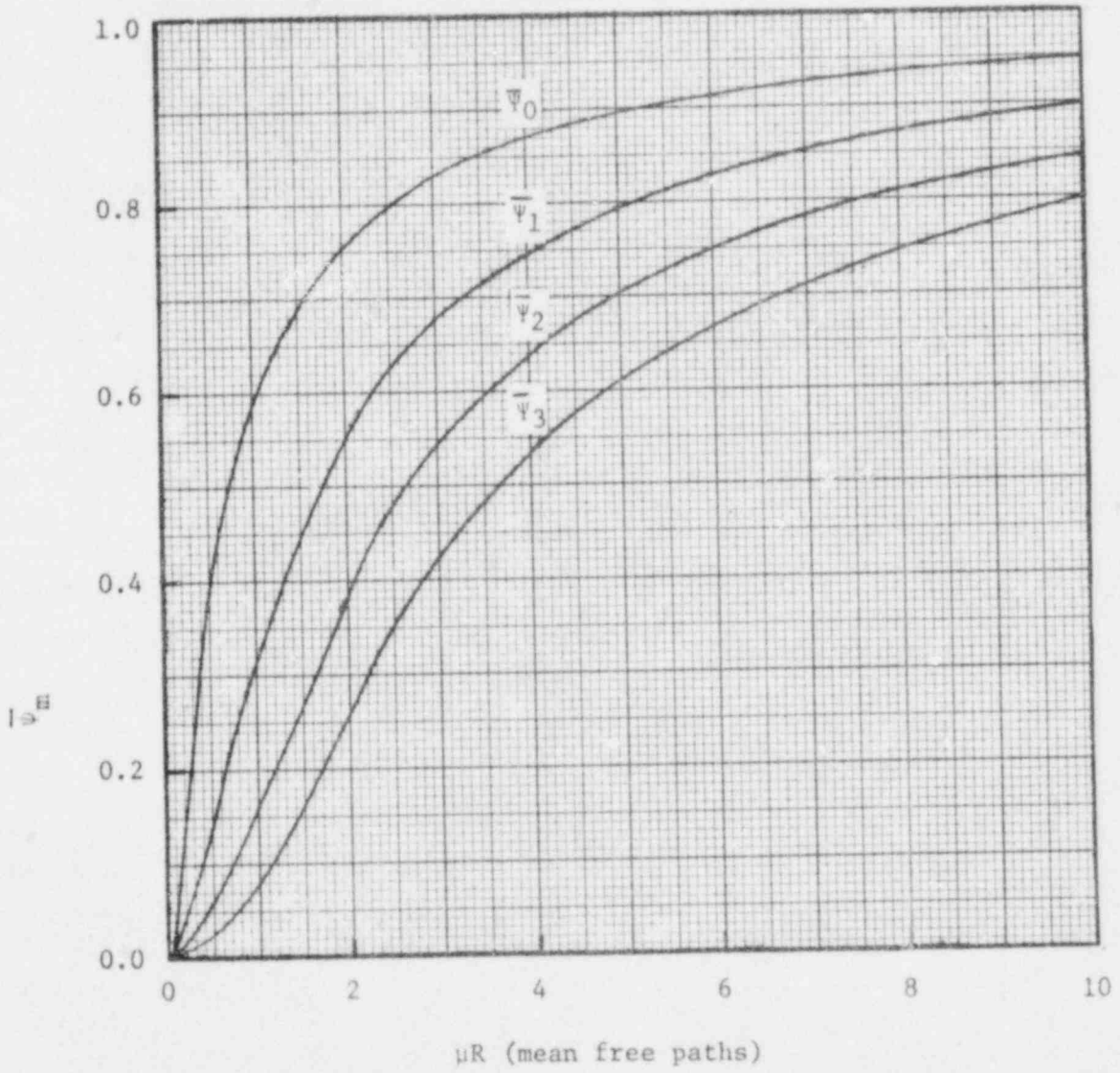

Fig. 3.1.1 Fuel rod segmentation and centroids

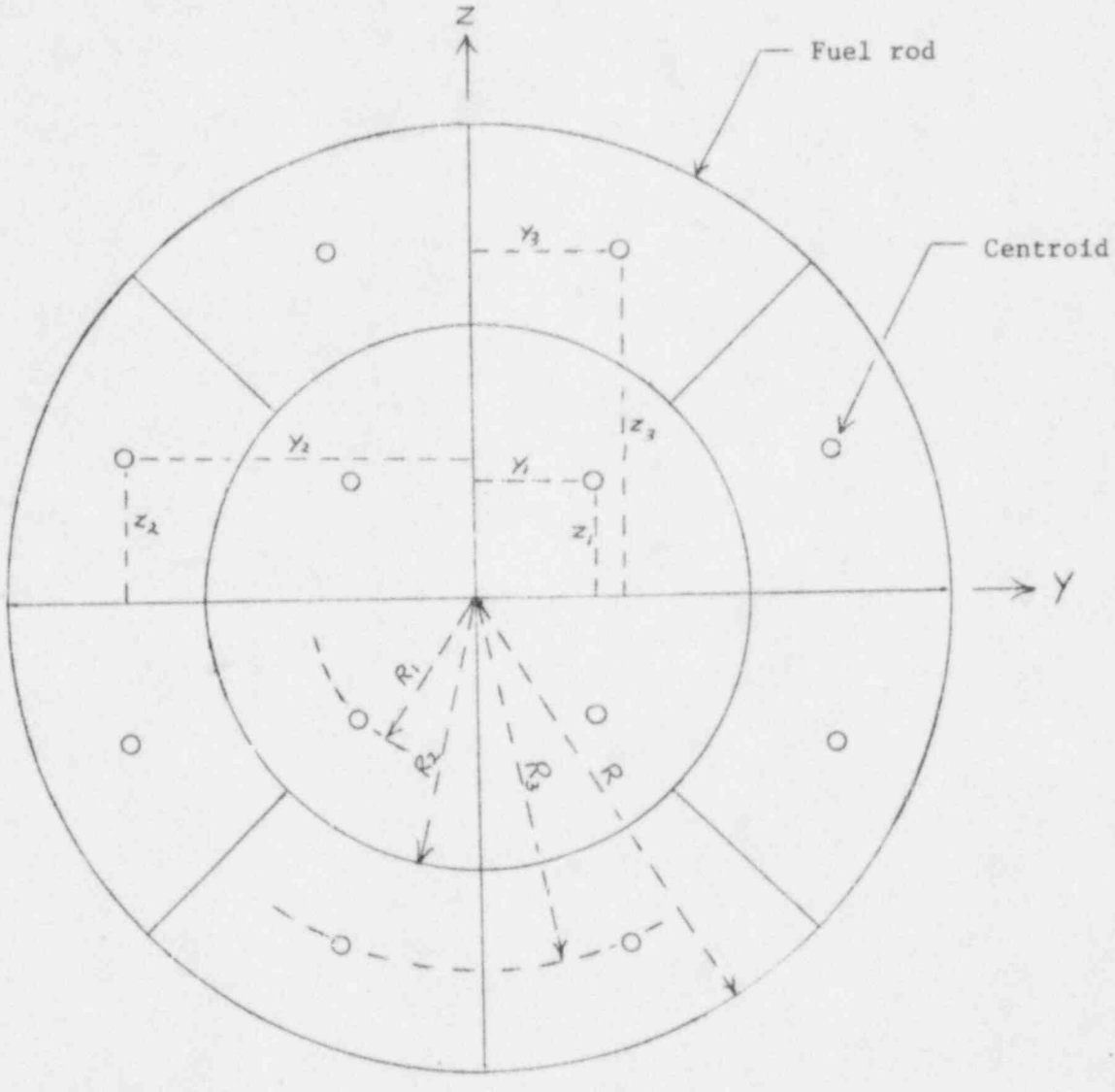

R = fuel rod effective radius

R_1 = 0.362R

R_2 = 0.577R

R_3 = 0.795R

Y_1 = 0.256R

Y_2 =-0.735R

Y_3 = 0.304R

$Z_1 = Y_1$, $Z_2 = Y_3$, $Z_3 = -Y_2$

Fig. 3.2.1 Yankee Rowe control rod configuration and region of interest

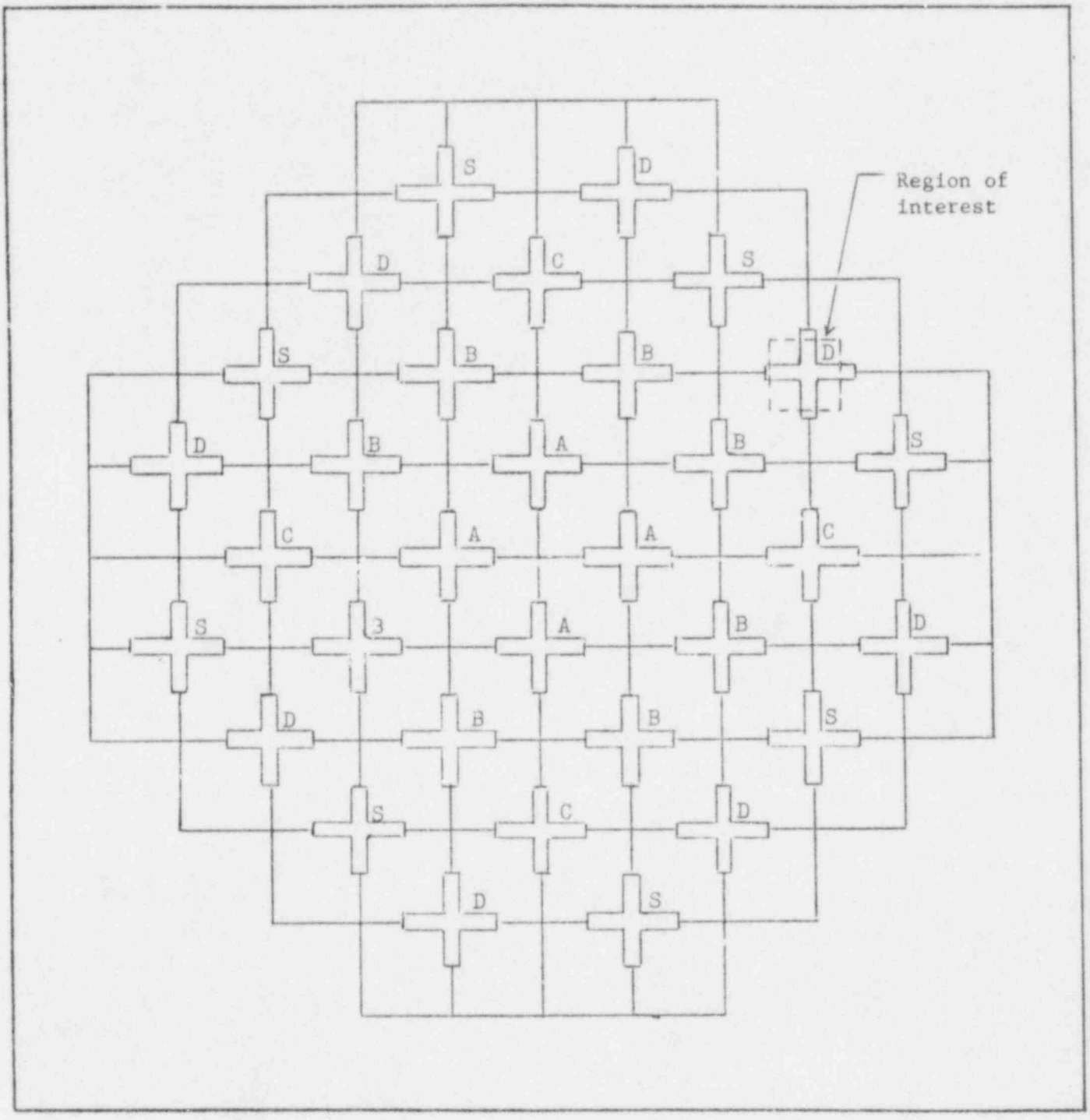

A - Regulating Rods

B - Used to attain power

C - Shutdown rods

D - Shutdown rods

S - Shim rods

Fig. 3.2.2 Core region analyzed and peaking factors

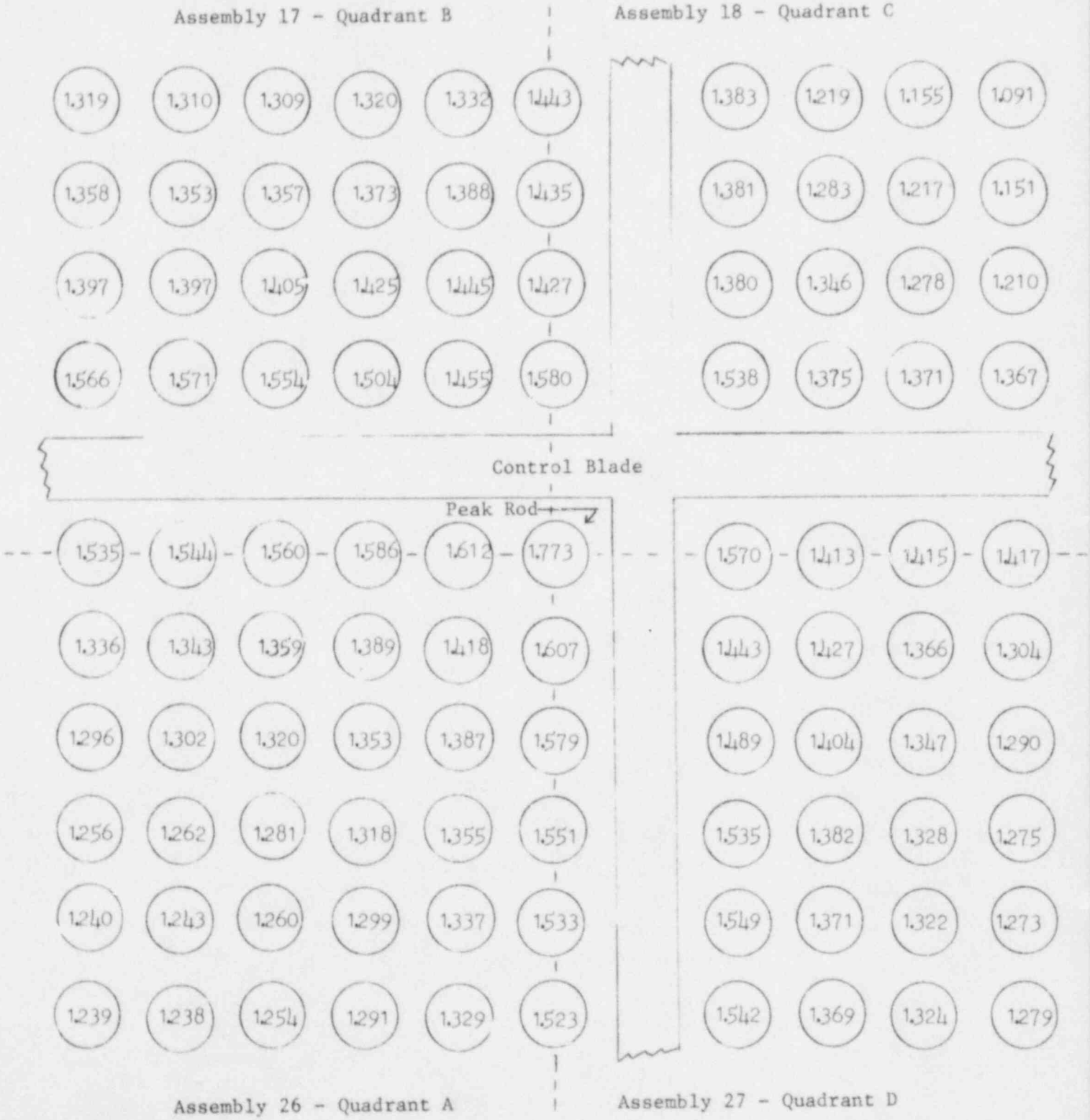

Fig. 3.2.3 Quadrant A representation for use with SHADRAC

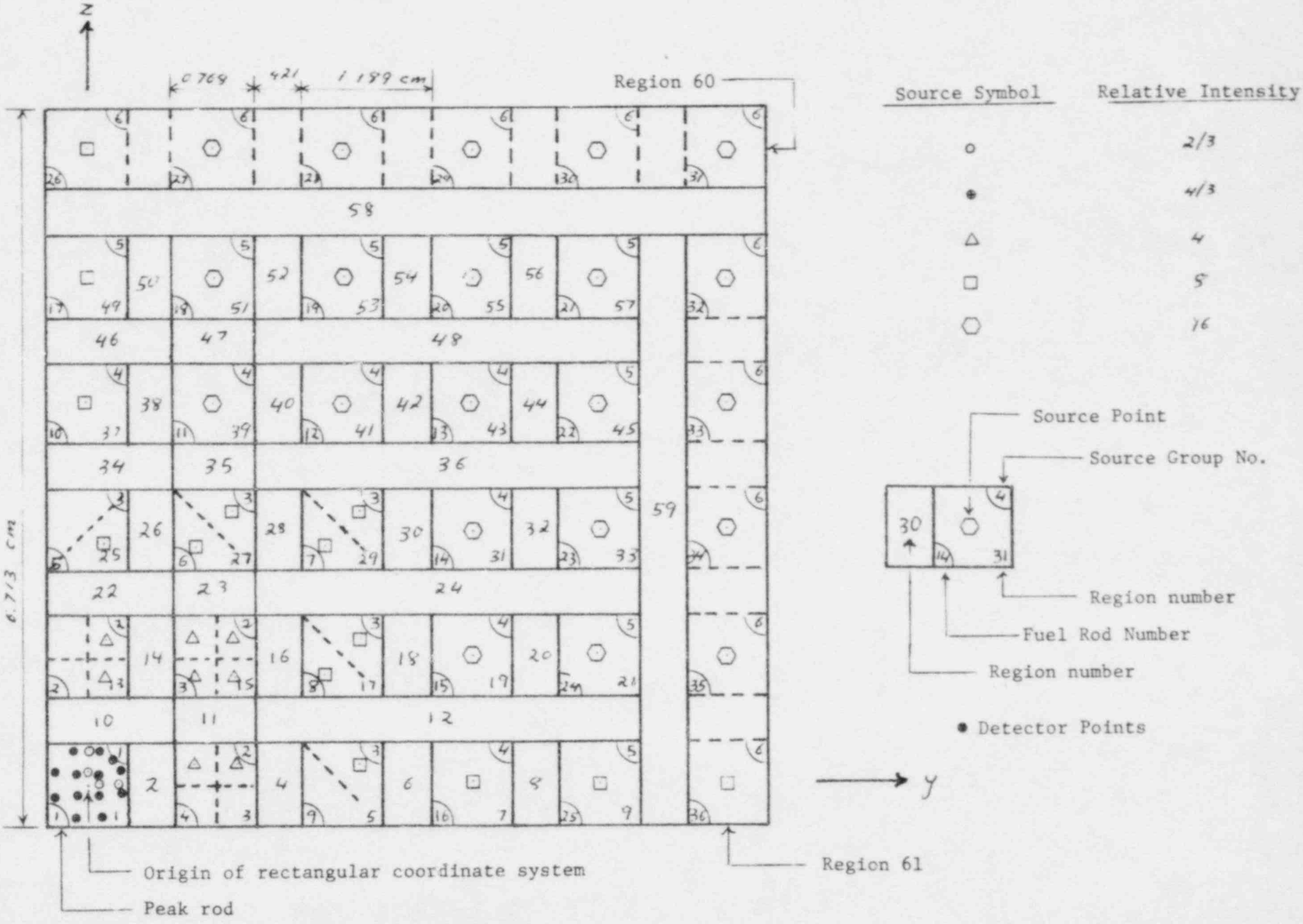

Fig. 4.2.1 Peak rod heating rate from point sources in 120 neighboring rods (uniform array/source intensity case)

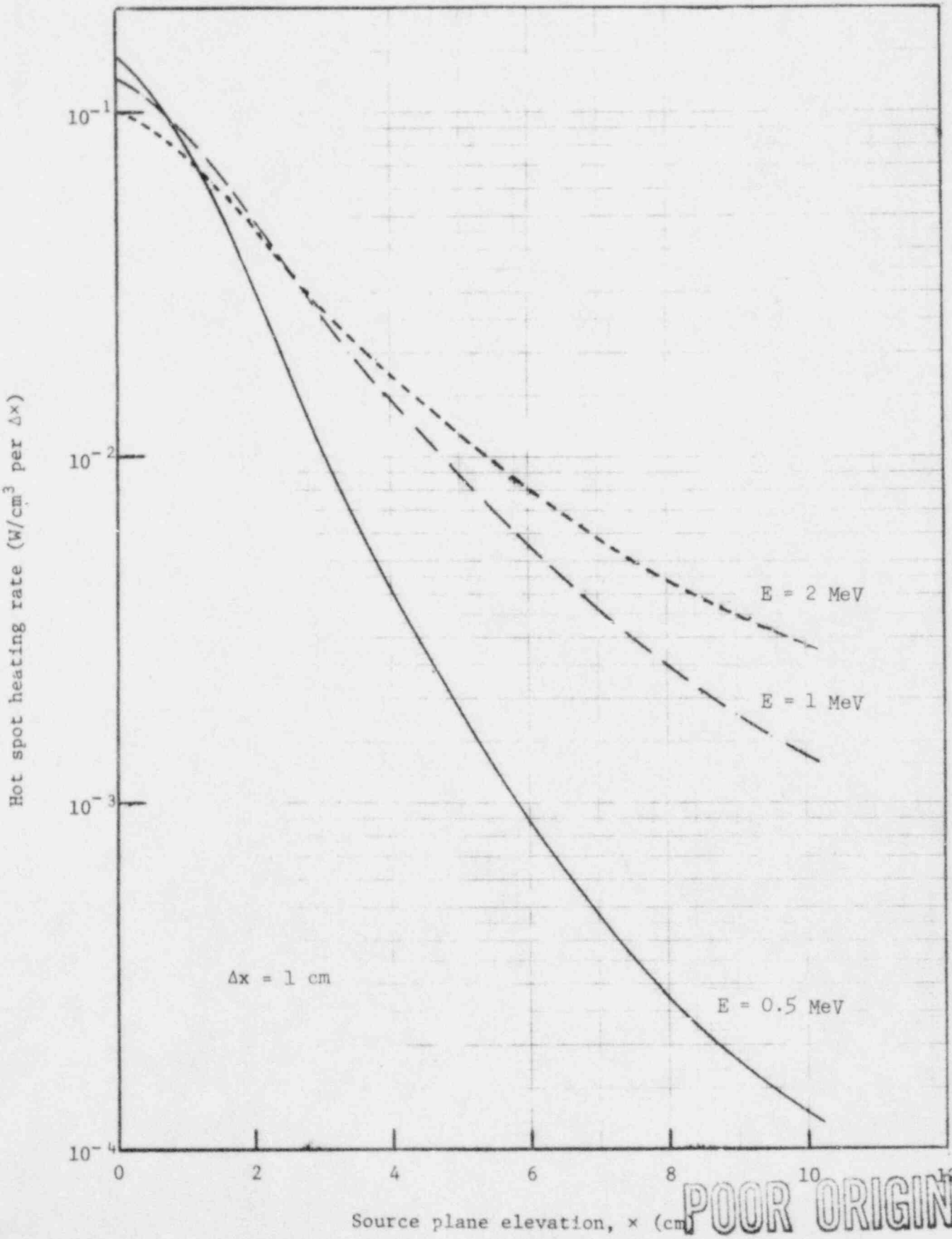

Fig. 4.2.2 Peak rod heating rate - Contribution from various source sets (uniform array/source intensity case)

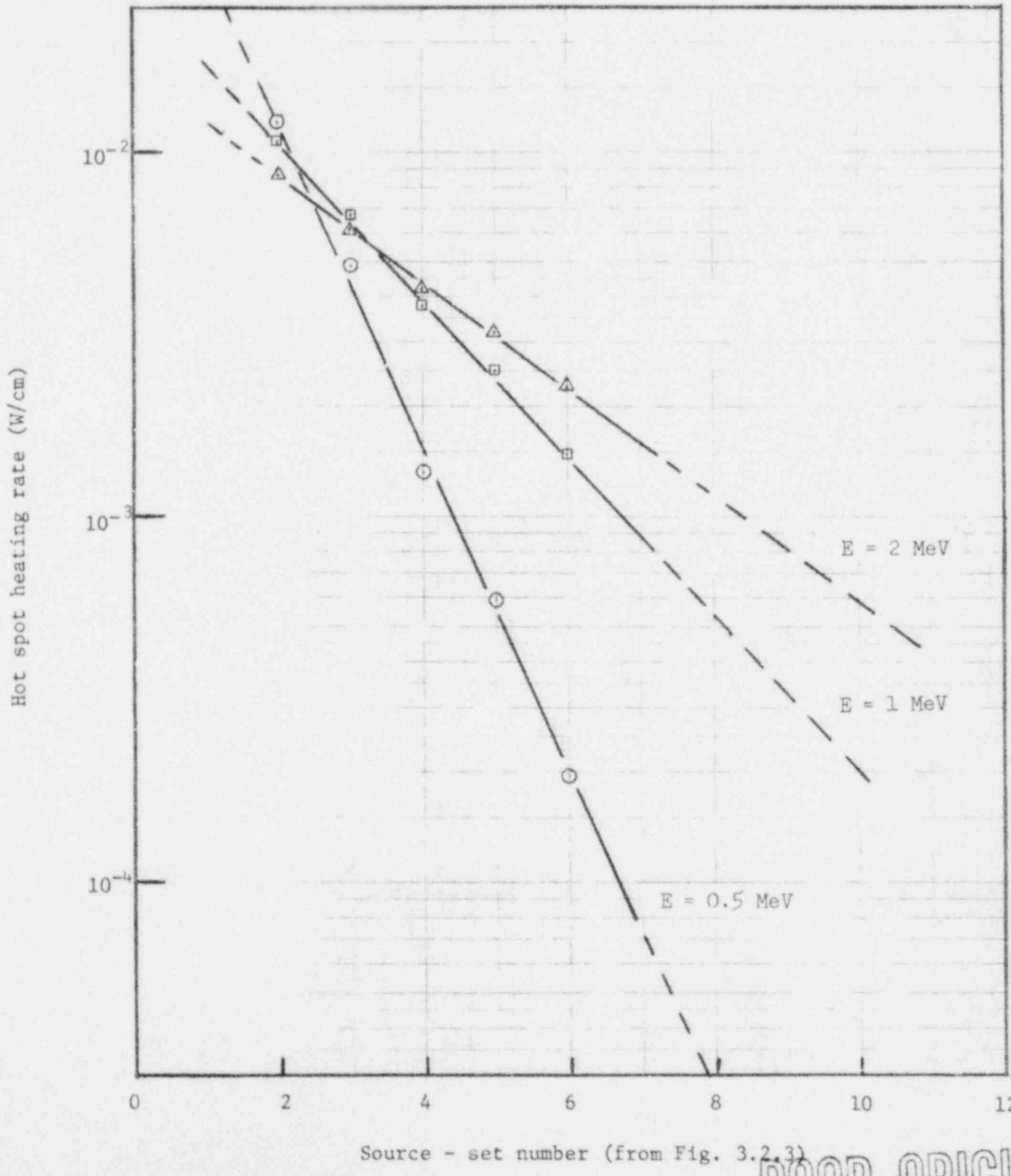

Fig. 4.3.1 Heat absorbed by peak rod
Monoenergetic gamma sources

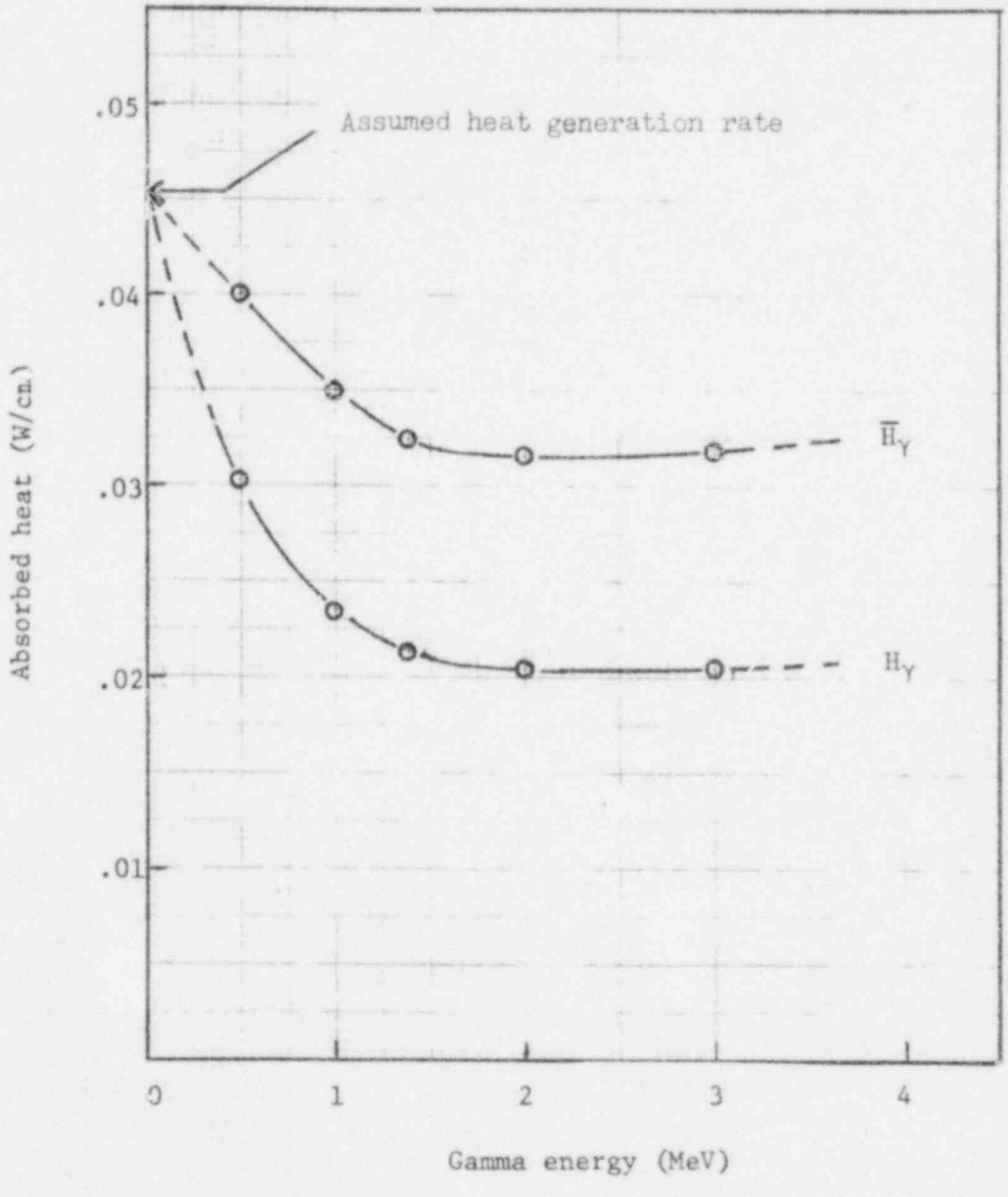

Fig. 4.4.1 Peak rod redistribution factors F_γ and F, and γ factor

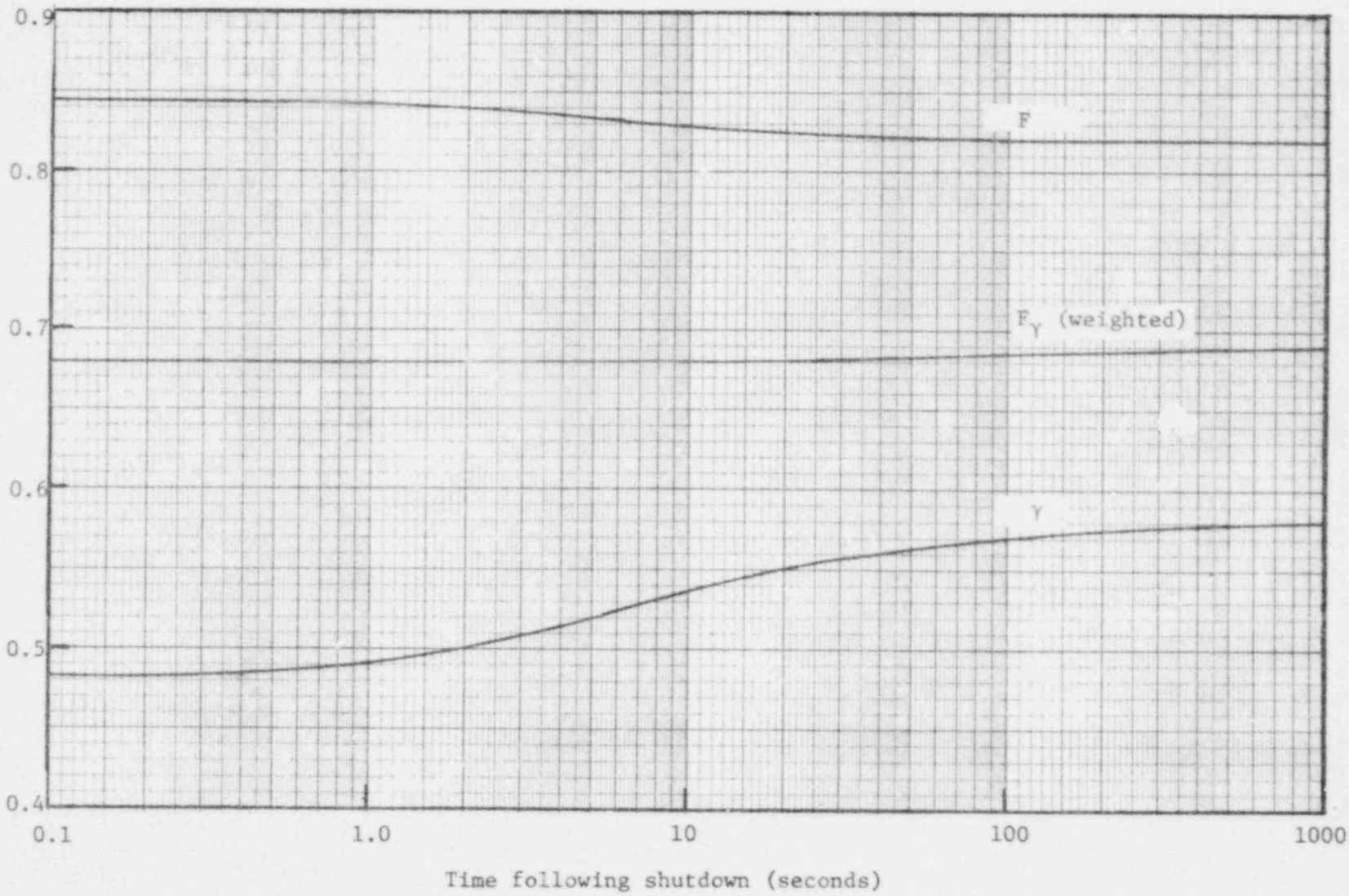

Fig. 4.6.1 Redistribution factors F_γ (top) and F (bottom) based on rule-of-thumb approach (γ = 0.482)

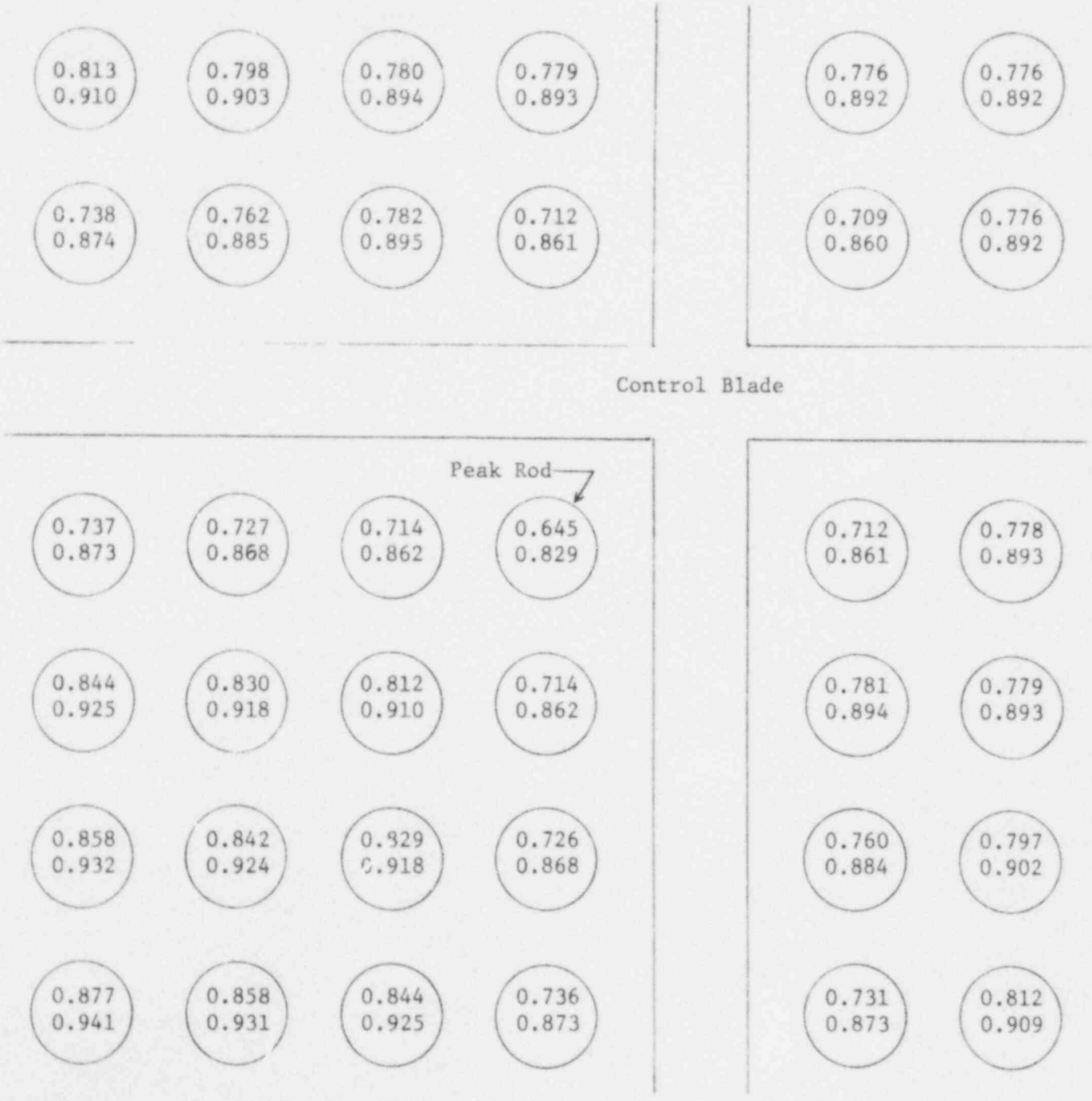

Fig. 4.6.2 Peaking factors before and after redistribution (rule-of-thumb model)

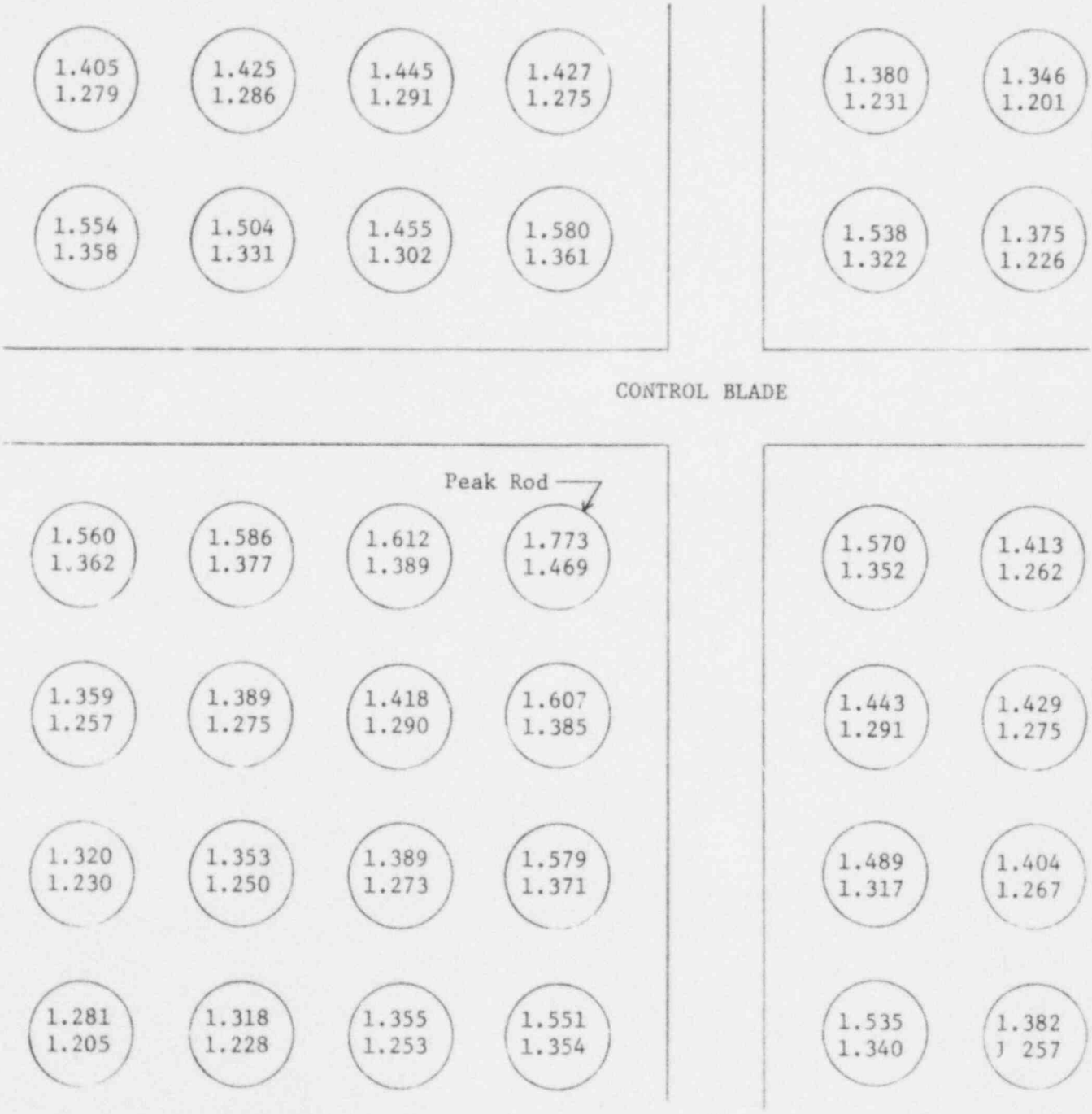

Fig. 4.6.3 Quadrant-A peaking factors before and after redistribution (rule-of-thumb model)